Nano Energy 66 (2019) 104167

Contents lists available at ScienceDirect

Nano Energy

journal homepage: http://www.elsevier.com/locate/nanoen

Full paper

Study of thin film blue energy harvester based on triboelectric nanogenerator and seashore IoT applications

Long Liu [a,b,c,d], Qiongfeng Shi [a,b,c,d], John S. Ho [a], Chengkuo Lee [a,b,c,d,e,*]

[a] Department of Electrical and Computer Engineering, National University of Singapore, 4 Engineering Drive 3, Singapore, 117576, Singapore
[b] Center for Intelligent Sensors and MEMS, National University of Singapore, Block E6 #05-11, 5 Engineering Drive 1, Singapore, 117608, Singapore
[c] Hybrid-Integrated Flexible (Stretchable) Electronic Systems Program, National University of Singapore, Block E6 #05-3, 5 Engineering Drive 1, Singapore, 117608, Singapore
[d] NUS Suzhou Research Institute (NUSRI), Suzhou Industrial Park, Suzhou, 215123, PR China
[e] NUS Graduate School for Integrative Science and Engineering, National University of Singapore, Singapore, 117456, Singapore

ARTICLE INFO

Keywords:
Liquid-solid contact triboelectric nanogenerator
Ū electrode
Blue energy harvester
Internet of Things (IoT)

ABSTRACT

Water wave energy, also known as blue energy, is a promising clean and renewable energy to solve global energy crisis. Recently, triboelectric nanogenerator (TENG) is considered as one of the most efficient approaches for harvesting water wave energy. Here we introduced a thin film blue energy harvester based on liquid-solid contact triboelectric mechanism. With novel external Ū electrode including a bar electrode (B electrode) and a U-shape electrode (U electrode), the shielding effect from water is hugely minimized, and outputs are effectively improved. Moreover, a series of IoT applications aiming seashore area is studied and realized, such as functions of wave level warning, continuously powering and a wireless signals transmission.

1. Introduction

In order to cope with the aggravating problem of energy supply and demand, lots of efforts focus on seeking renewable and clean energy source, such as solar energy, wind energy, ocean energy and so on [1–3]. When compared with other mentioned energies, the ocean energy, also called blue energy, covering over 70% of the Earth's surface, contains abundant energy and shows advantage of less dependence on weather, seasonality, and day-night rhythm [4,5]. The blue energy is mainly in forms of wave energy, tidal energy, thermal energy and osmotic energy. And the wave energy around the globally coastline has reach more than 2 TW according to the estimation [6–9]. Current approaches of harvesting wave energy are based on bulky and costly electromagnetic generator. According to different practical application scenarios from shoreline to far offshore area, different kinds of devices have been equipped, such as limpet (Oscillating water column), Oyster (Oscillating wave surge converter), Wave dragon (Overtopping device), Ocean energy (Oscillating water column), WaveBob (Oscillating point absorber) and Pelamis (Line attenuator) [10,11]. However, due to their complex hydraulics and mechanical structures applied in the electromagnetic generator to transform wave motion into linear reciprocal motion or rotary motion, the electromagnetic generator suffers from disadvantages of big-size, heavy-weight and high-cost, limiting them to be applied in large-scale wave energy harvesting, especially at low frequency [12].

Recently, the emergence of triboelectric nanogenerator (TENG) has brought a new route for harvesting wave energy [13–18]. The triboelectric nanogenerator's origin can be derived to Maxwell's displacement current, and its operating principle is based on the conjugation of triboelectric effect and electrostatic induction [19–22]. This new technology has been considered as one of the most promising ways to harvest ambient mechanical energy with unique merits of easy-fabrication, low-cost, lightweight, and environment-friendly. Former works have proved that the triboelectric nanogenerator can effectively convert mechanical energy with various forms into electric energy, such as human motions [23–31], mechanical vibration [32–36], natural wind [37–39], water drops [40–46] and water waves [47–73]. Among kinds of water wave energy harvesters, the fully enclosed rolling spherical structure is mostly studied since it can harvest the energy from all directions. Wang et al. have applied a Nylon ball rolling on a Kapton film with two stationary back electrodes attached to the inner surface of the spherical shell [47]. Xu et al. have applied a soft silicone rubber rolling in the sphere so that the effective area for triboelectrification was

* Corresponding author. Department of Electrical and Computer Engineering, National University of Singapore, 4 Engineering Drive 3, Singapore, 117576, Singapore.
E-mail address: elelc@nus.edu.sg (C. Lee).

https://doi.org/10.1016/j.nanoen.2019.104167
Received 20 August 2019; Received in revised form 19 September 2019; Accepted 4 October 2019
Available online 9 October 2019

increased due to more intimate contact [48]. Compared with traditional electromagnetic generator, the triboelectric nanogenerator effectively adapts in transforming mechanical energy of random and low frequency into electric power, so that the triboelectric nanogenerator is appropriate for harvesting energy from low-frequency waves [74–76].

Various kinds of devices have been developed and applied in harvesting wave energy, and it can be divided into two types: liquid–solid contact mode device [49–57,59] and solid–solid contact mode device [60–72]. Wherein solid-solid contact mode device with encapsulated package outside attracted a large proportion of research attentions, because outputs of triboelectric nanogenerator are greatly influenced by environmental conditions especially humidity [77–80]. These devices with different encapsulated structures, such as spheres [61–63], boxes [64,65], cylinder structure [69–71], Pelamis snake structure [67] and oblate spheroidal structure [68], need float on water so that only suit for far offshore area. In general, these rigid encapsulated structures will make whole device large-size and weight-increase. Moreover, strict requirements for waterproof level increase the difficulty of further industrial production, recovery and maintenance. In contrast, liquid-solid contact mode device could be smaller size even be thin-film type device, which can be readily integrated with most of the current infrastructures [50–54]. Zhu et al. have proposed a series of works about thin-film type devices applying array of electrodes underneath dielectric film to utilize dynamic changed electrical double layer to harvest wave energy [50–52]. These thin-film type devices can be applied as blue energy harvester in seashore area by being fixed on shoreline, and in far offshore area by being attached on floating workstation or boats. When water waves repeatedly submerge devices, these liquid-solid contact mode triboelectric nanogenerators can convert wave energy into electric power by utilizing surface triboelectric charges generated through the interaction with water waves and dielectric film. Other kinds of liquid-solid contact mode triboelectric nanogenerators like ball structure [49], buoy-like structure [55] and tube structure [56] are also applied to harvest wave energy and collect waves' information, and these kinds of device can be applied in far offshore area. Therefore, the liquid-solid contact mode triboelectric nanogenerator shows a great potential to serve as a blue energy harvester in expansive sea area.

However, the shielding effect limits outputs of the TENG device when it is operated with water waves [58]. This shielding effect attributes to the electrical double layer (EDL) formed on interface of solid device and liquid water environment [81,82]. The EDL refers to two parallel layers of charges surrounding the interface. The first layer, also called as the stern layer, consists of anchored ions attracted onto the solid surface. The second layer, also called as diffuse layer, is composed of free ions which are loosely associated with the solid and can move with the liquid. This second layer will electrically screen the first layer due to loosely counter ions. To minimize the shielding effect from water, Zhang et al. report a extra airgap structure applied in solid-solid contact triboelectric nanogenerator device, which utilizes rolling polytetrafluroethylene balls and is based on freestanding triboelectric-layer mode [67]. Xu et al. report tube structure with airgap applied in liquid-solid contact triboelectric nanogenerator device, which utilizes an acrylic tube attached a PTFE film with electrode and is based on single-electrode mode [56]. Finally, the outputs of these devices are improved with the extra airgap structures. Thus, it can be seen the importance of dealing with the shielding effect.

In addition, considering rapidly increased requirement to the Internet of Things (IoT), the triboelectric nanogenerator shows a great potential in this application as self-powered sensors for IoT system [83]. Although self-powered sensors based on triboelectric nanogenerator have been applied in Smart Home System [27,28,84–86], Wearable Technology [26,45,87] and Human-Computer Interaction Techniques [29–31], rare research works are discussed Seashore IoT Applications with triboelectric nanogenerator. On one hand, the thin film typed triboelectric nanogenerator suits for seashore area. On the other hand, triboelectric nanogenerator based on liquid-solid contact mode can obtain immediate signals due to its direct operation with water waves.

Here we introduce a thin film blue energy harvester based on liquid-solid contact triboelectric nanogenerator. The structure of final device is flexible and bendable, suitable for substrate with various surfaces and situations. First, with novel external $\bar{U}$ electrode including a bar electrode (B electrode) and a U-shape electrode (U electrode), the shielding effect is significantly minimized, and outputs are effectively increased. Second, the liquid-solid contact triboelectric mechanism with external $\bar{U}$ electrode is studies in details, and separated influence of B electrode and U electrode are experimental discussed. Third, in further applications in seashore IoT system, the U electrode can extract power from waves' flood and ebb processes and the B electrode can work as a safety switch, then whole device can form a wave warning system and provide continuous power supply to the normal operation of a temperature sensor. Finally, a wireless transmitter is powered with the $\bar{U}$ electrode and successfully sends out the environment information to a mobile phone. Therefore, this work provides a new kind of thin film blue energy harvester propitious to industrial production and expands its applications in IoT area.

2. Results and discussion

2.1. Structure and working principle of the $\bar{U}$ electrode triboelectric nanogenerator

A schematic diagram of the $\bar{U}$ electrode triboelectric nanogenerator ($\bar{U}$-TENG) for harvesting water wave energy around coastline is shown in Fig. 1. And the structure design and fabrication process of $\bar{U}$-TENG is shown in Fig. 1a, which is also illuminated in experimental section. As can be seen from upper part of Fig. 1a, the structure is suitable for stack fabrication process and has potential of further scale-up industrial production. The prepared device is displayed in Fig. 1b, and the bended part proves its flexibility and thin-film characteristics. By the abridged general view and the prepared device's photo, the Bar electrode (B electrode), Dielectric electrode (D electrode) and U-shape electrode (U electrode) are obviously clarified. Moreover, flow chart diagram of IoT applications (Fig. 1c) proposes that the $\bar{U}$-TENG can be placed on seashore and applied as blue energy harvesters. Converted wave energy can be utilized to support IoT applications in seashore area, and details will be discussed in below section.

The $\bar{U}$-TENG is developed from dielectric electrode triboelectric nanogenerator (D-TENG), and the D-TENG belongs to the single-electrode mode of four basic working modes [18,19]. Besides different structure shown in Fig. 2a, the D-TENG and the $\bar{U}$-TENG have distinct working principles and outputs. Details are shown in Fig. 2b and c, where their working principles are based on cross sectional view. The first thing should be clarified is the electrical double layer (EDL) formed on the interface between dielectric film and water waves. When water wave starts moving forward onto the dielectric film's surface, the surface groups may lead its surface to be negative charged, and the electrical double layer will be formed to neutralize these surface charges [55–58]. The EDL part consists of a Stern layer and a diffuse layer, related schematic diagram is shown in Fig. S1. The Stern layer refers to ions adsorbed onto the dielectric surface. The diffuse layer contains mobile ions which are loosely associated with the solid and can move with water wave. More moveable ions are there in the diffuse layer, more heavily the charges on the dielectric surface are screened. And then outputs of liquid-solid contact mode triboelectric nanogenerator are influenced [55,57].

For the D-TENG shown in Fig. 2b, its working mechanism can be divided into following steps: (i) The new cycle starts with the dielectric film is pre-charged with negative charges due to preliminarily friction with water waves, and loosely positive and negative ions are distributed in water environment. (ii) When water wave starts contacting with the dielectric film, the EDL will be formed on the interface, wherein positive ions are attracted to form the first layer and several loosely negative ions

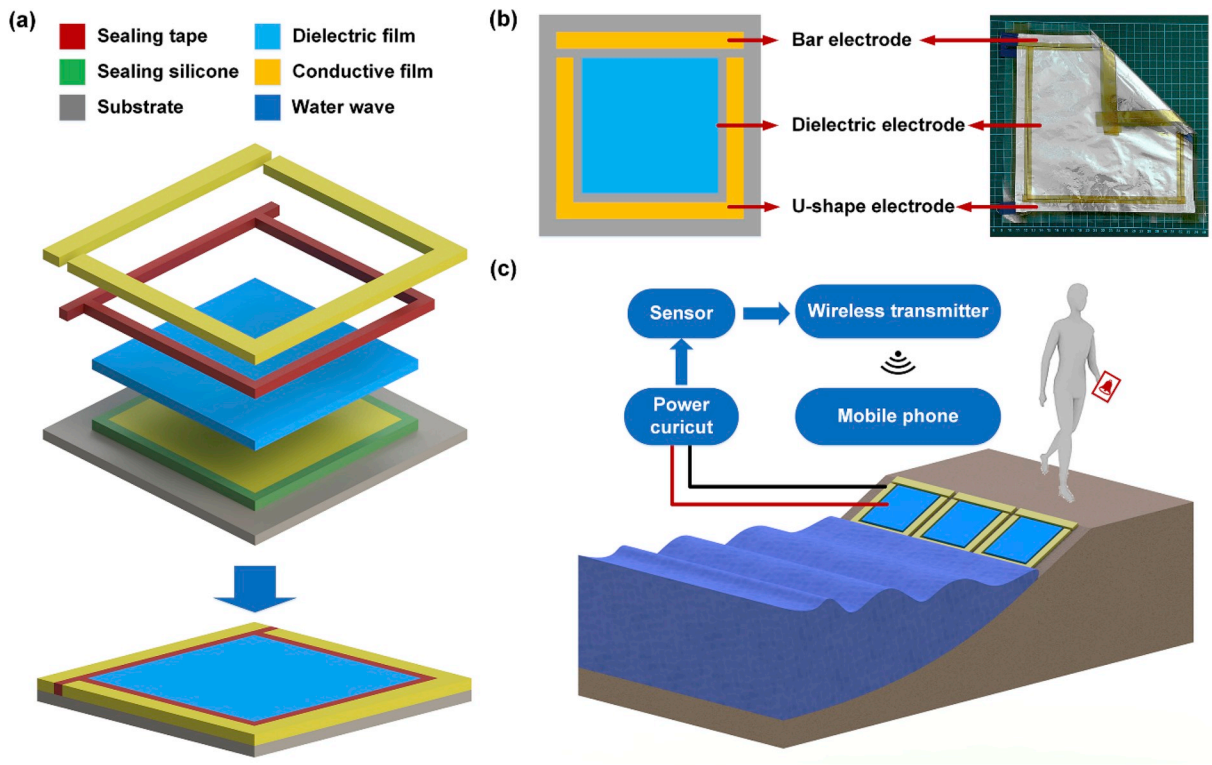

Fig. 1. (a) The structure design and fabrication process of the Ū electrode triboelectric nanogenerator (Ū-TENG). (b) Schematic diagram of the abridged general view (left) and prepared device's photo (right). (c) Flow chart diagram of applications of Ū-TENG as blue energy harvester.

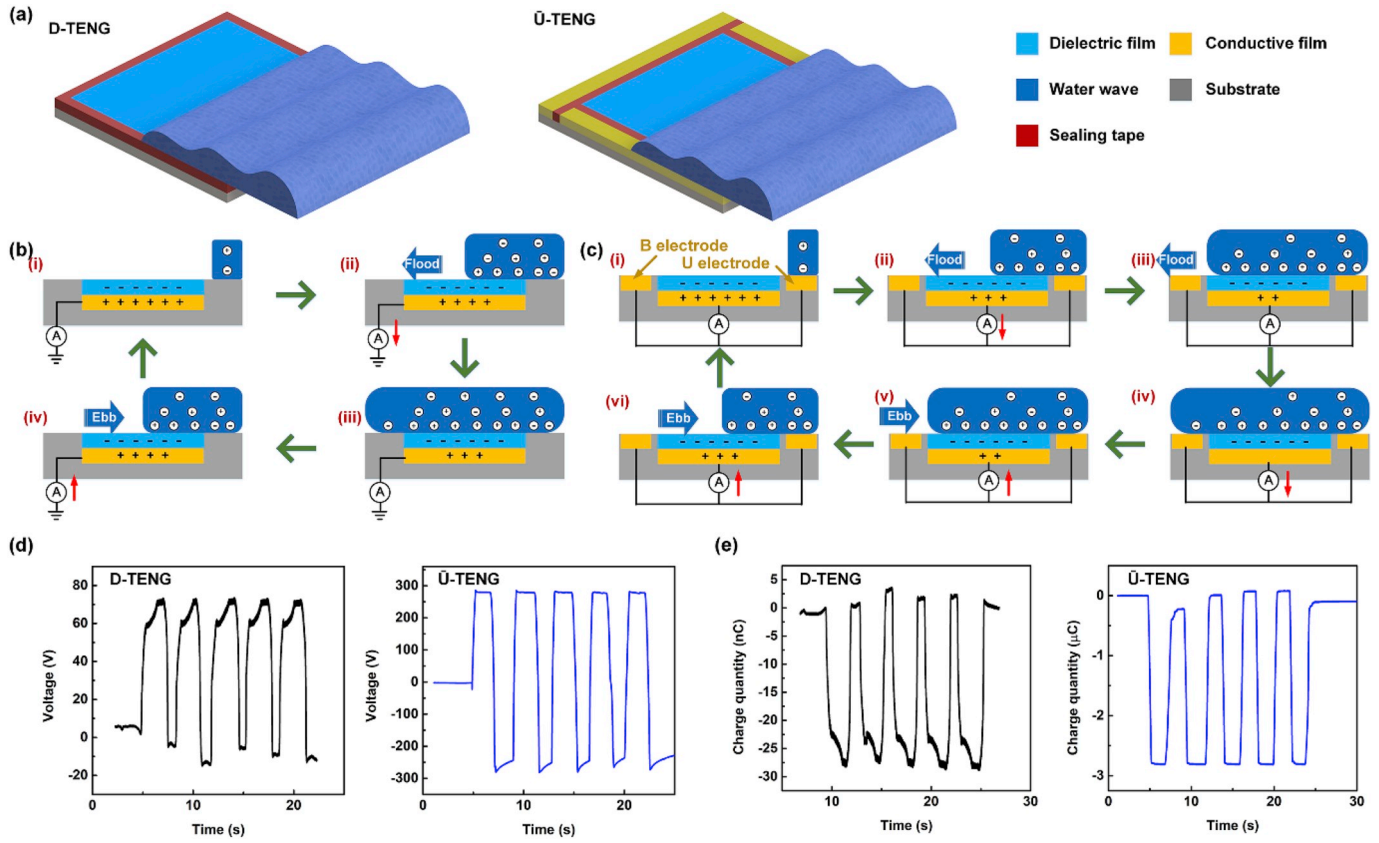

Fig. 2. (a) The structure of the D-TENG and the Ū-TENG. (b) Work mechanism of the D-TENG. (c) Work mechanism of the Ū-TENG. (d) Open-circuit voltage comparison of the D-TENG and the Ū-TENG. (d) Transfer charge quantity comparison of the D-TENG and the Ū-TENG.

moved with water wave form the second layer. Overall, equilibrium of electrical neutrality in the initial state is disturbed, and electrical signals are generated in external circuit and flow to the ground. (iii) Along with the disturbed equilibrium, the EDL is gradually submerge the dielectric film until it is complete covered. And new equilibrium of electrical neutrality is built with the EDL. (iv) When the water wave breaks down and start leave the dielectric film, influence of the EDL also recedes and electrical signals are generated in external circuit and flow to the dielectric electrode. At the end of the cycle, the water wave is completely away and back to the initial state of (i). This working mechanism shows that there will be less charges flow in the external circuit attributed to the shielding effect from water, resulted in low outputs of the D-TENG.

Above all, the loosely negative ions in the second layer screen the charges on the dielectric surface and will limit outputs of the triboelectric nanogenerator. The Ū-TENG utilize external Ū electrode (include Bar electrode and U-shape electrode) to minimum this shielding effect from the second layer, and its working mechanism is explained in Fig. 2c, where can be divided into following steps: (i) The cycle starts with the dielectric film is pre-charged with negative charges due to preliminarily friction with water waves, and loosely positive and negative ions are distributed in water environment. (ii) When water wave once contacts with U electrode, loosely ions are influenced with electric potential difference between the D electrode and U electrode, and negative ions are inclined to retained in the water area away from D electrode. For the liquid-solid contact area, the EDL formed to reach new equilibrium of electrical neutrality. Overall, along with motion of water wave, initial equilibrium is constantly disturbed, then electrical signals are generated in external circuit and flow from D electrode to U electrode. (iii) When the water wave completely covers the area of D electrode and U electrode, a temporary equilibrium is achieved between the D electrode and U electrode. For the EDL formed on the interface of liquid-solid contact area, there may still exist loosely negative ions in the second layer. (iv) After the water wave across the D electrode and the U electrode, the water wave contacts with the B electrode, remained loosely negative in the second layer can further attracted to the B electrode due to electric potential difference from D electrode, thus electrical signals are generated in external circuit and flow from D electrode to B electrode. When water wave fully covers the device, new equilibrium of electrical neutrality is built with the EDL. (v) Then, after flood process, the water wave starts ebb away from the device. The loosely ions absorbed on B electrode will move away with the water wave. Thus, equilibrium of electrical neutrality is broken, and then electrical signals are generated in external circuit and flow from B electrode to D electrode. (vi) Then the water wave starts ebb away from area of D electrode. The equilibrium is continuously broken, and electrical signals in external circuit flow from U electrode to D electrode until water wave completely away from the device. Then the cycle is back to the initial state of (i).

Compared with the D-TENG, the Ū-TENG is less affected with the shielding effect from the water. Because the U electrode and B electrode attracted these loosely ions and exclude their screen influence on charges in dielectric film. Related proofs are shown in Fig. 2d and e, and Fig. S2, where comparisons of outputs between the D-TENG and the Ū-TENG are discussed. Open-circuit voltage increases from 73.1 V to 283.1 V, transfer charge quantity increases from 28.4 nC to 2.8 μC and short-circuit current increases from 0.4 μA to 10.8 μA. Overall, the Ū electrode including B electrode and U electrode plays a key role to minimize the shielding effect and enhance the outputs. Another advantage of the Ū electrode should be noted about dynamic change of water film on liquid-solid interface in ebb process [88,89]. Shown in the Video S1, although water waves are directional, broken processes of water film are unpredictable due to complex and environment. The surface energy in the water film can be extracted by the Ū electrode, whatever orientation the water film will break away. Therefore, the Ū-TENG can be effectively applied as blue energy harvester and convert wave energy into electric power.

Supplementary data related to this article can be found at https://doi.org/10.1016/j.nanoen.2019.104167.

2.2. Functions and output performance of bar electrode and U-shape electrode

As above mentioned, the Ū electrode consists of Bar electrode (B electrode) and U-shape electrode (U electrode). When the Ū-TENG operates with water waves, B electrode and U electrode play with synergistic mechanism. Next part will discuss functions and outputs of these two electrodes respectively, and triboelectric nanogenerator with U electrode or B electrode is defined as U-TENG or B-TENG.

Up for the U-TENG, its schematic diagram of front view is shown in Fig. 3a, where U electrode and D electrode access external circuit. As shown in Fig. 3b, c and d, average open-circuit voltage reaches 256 V, average transfer charge quantity reaches 2.46 μC and average short-circuit current reaches 9.8 μA. Although these outputs of U-TENG are slightly lower than the Ū-TENG, results show an equal order of magnitude and prove ability of blue energy harvester. As for practical application, rectifier circuit is needed, and rectified current is shown in Fig. 3e. Average rectified current 15.2 μA, and this amount of increase is attributed to complexity of liquid-solid interaction. Next, capacitors of 1 μF, 4.7 μF, 10 μF, 47 μF and 100 μF are applied to store converted electric power. After five cycles of flood and ebb process with 0.25 Hz, final voltage for capacitor can reach 19.72 V, 4.98 V, 2.31 V, 0.51 V and 0.21 V respectively.

Same tests are performed with the B-TENG, its schematic diagram of front view is shown in Fig. 4a, where B electrode and D electrode access external circuit. As shown in Fig. 4b and c, average open-circuit voltage reaches 211.2 V, average transfer charge quantity reaches 2.34 μC. However there exist a huge difference on the short-circuit current between flood process and ebb process. Average short-circuit current in flood process can reach 0.44 mA, but average short-circuit current in ebb process is only 1.25 μA. This difference is attribute to the water wave is instantaneously contact and non-contact with B electrode, and B electrode plays as a conceptive switch in external circuit. Thus, B electrode can be applied as a safety switch in a wave warning system, which will be discussed in below part. Rectified current is tested and shown in Fig. 4e and mentioned difference in flood and ebb process is also shown. Next, capacitors of 1 μF, 4.7 μF, 10 μF, 47 μF and 100 μF are applied to store converted electric power. After five cycles of flood and ebb process, final voltage for capacitor can reach 18.86 V, 4.81 V, 2.27 V, 0.5 V and 0.21 V respectively. Compared with the performance of U electrode, charged voltage is slightly lower, because that operation of B electrode is instantaneous.

Moreover, output powers of U electrode and B electrode are discussed in Fig. 5. For U-TENG, dependence of voltage and current in the flood process and the ebb process are shown in Fig. 5a and b. Obviously, both in the flood process and the ebb process, average voltage rises exponentially with the external resistance load and then gradually saturates. And the corresponding current drops with the external resistance load. The average output power of U-TENG with error bar is shown in Fig. 5c. The results show that the average power in the flood process reaches the maximum value of 358.93 μW at external resistance load of 10 MΩ. The average power in the ebb process reaches the maximum value of 1.51 mW at external resistance load of 53 MΩ. These different values of output power in the flood and ebb process are attributed to the released surface energy which is collected with U electrode. For B-TENG, dependence of voltage and current in the flood process and the ebb process are shown in Fig. 5d and e. The overall trend of voltage is increasing with the external resistance load. And corresponding current's general trend is dropping with the external resistance load. The average output power of B-TENG with error bar is shown in Fig. 5f. The average power in the flood process reaches the maximum value of 30 mW at external resistance load of 100 kΩ. And the average power in the ebb process reaches the maximum value of 463.51 μW at external

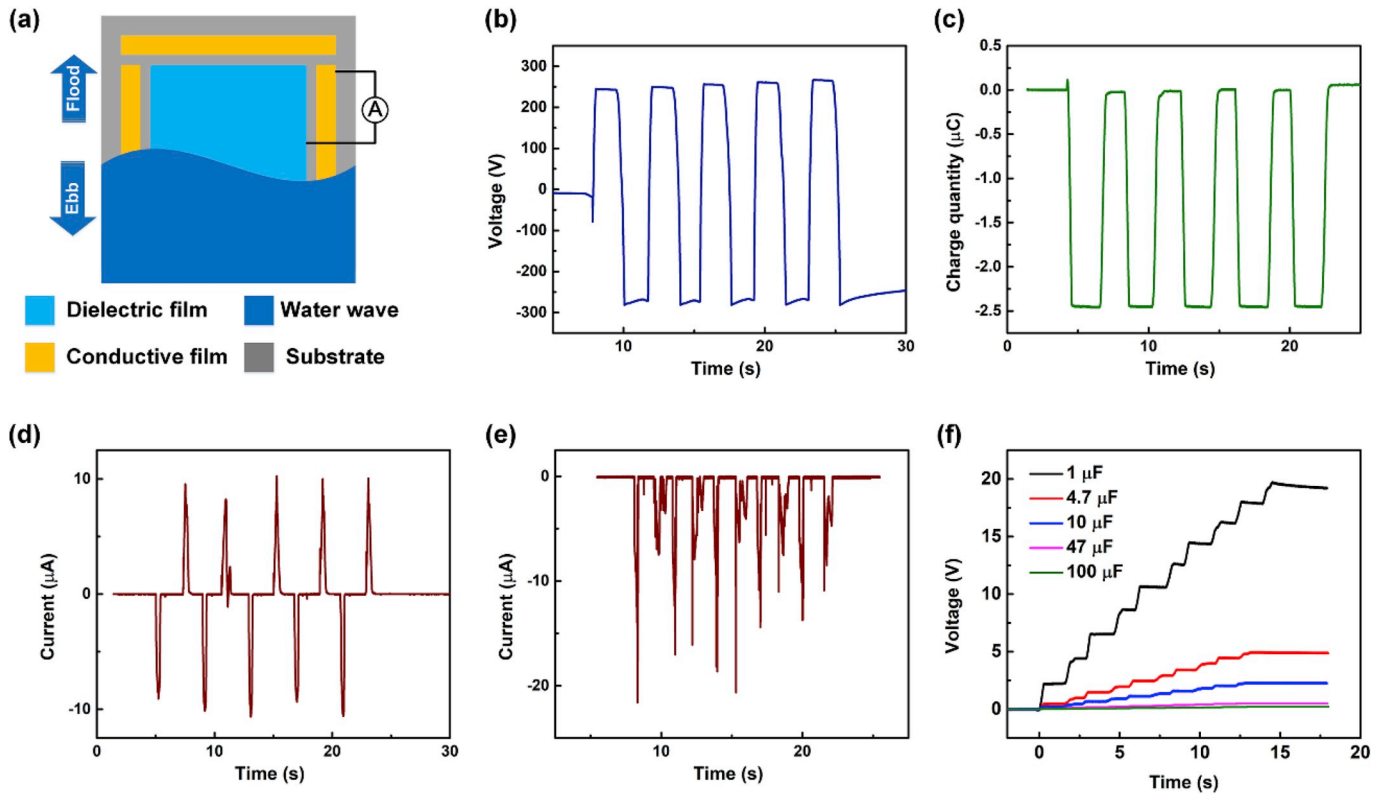

Fig. 3. (a) The schematic diagram of front view of U-TENG. (b) Open-circuit voltage of U-TENG. (c) Transfer charge quantity of U-TENG. (d) Short-circuit current of U-TENG. (e) Rectified current of U-TENG. (f) Capacitor charge with U-TENG.

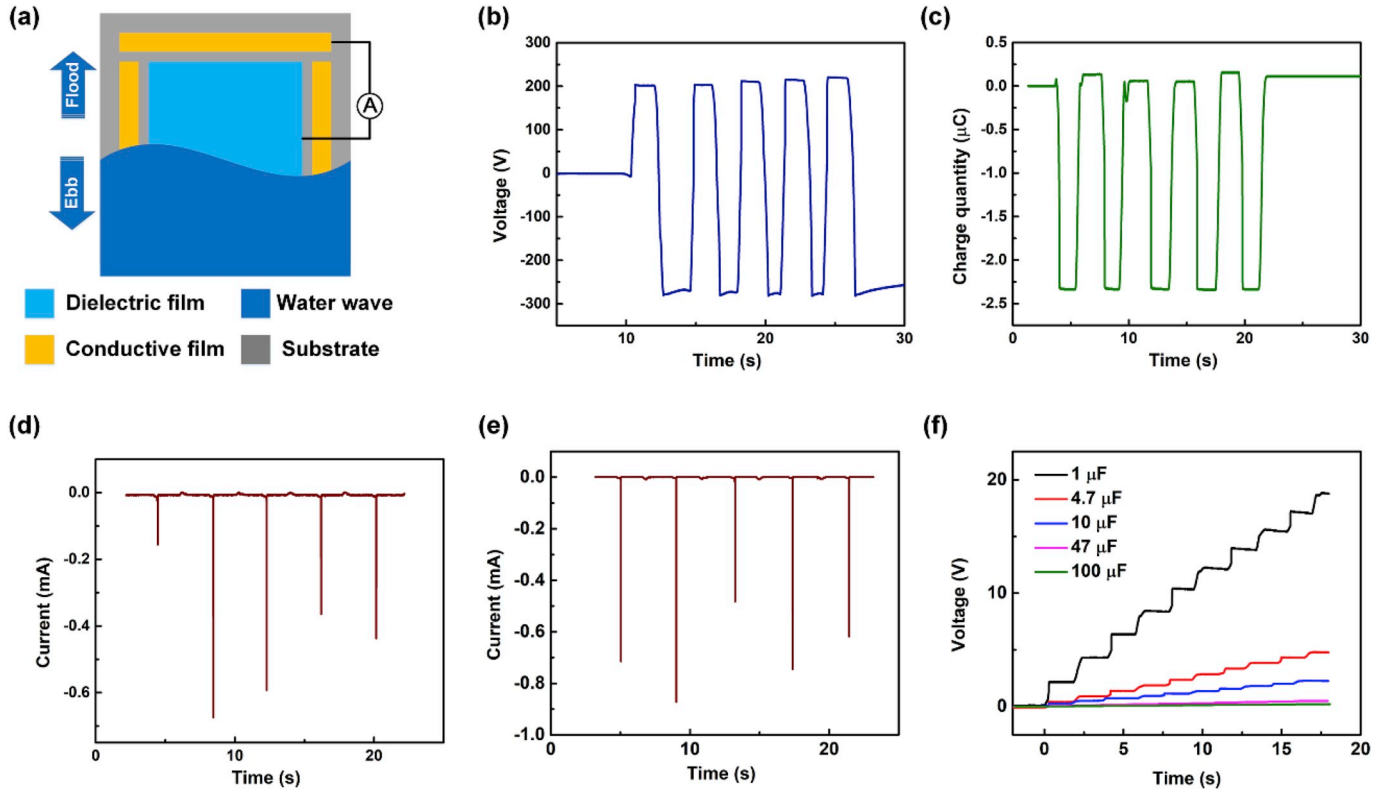

Fig. 4. (a) The schematic diagram of front view of B-TENG. (b) Open-circuit voltage of B-TENG. (c) Transfer charge quantity of B-TENG. (d) Short-circuit current of B-TENG. (e) Rectified current of B-TENG. (f) Capacitor charge with B-TENG.

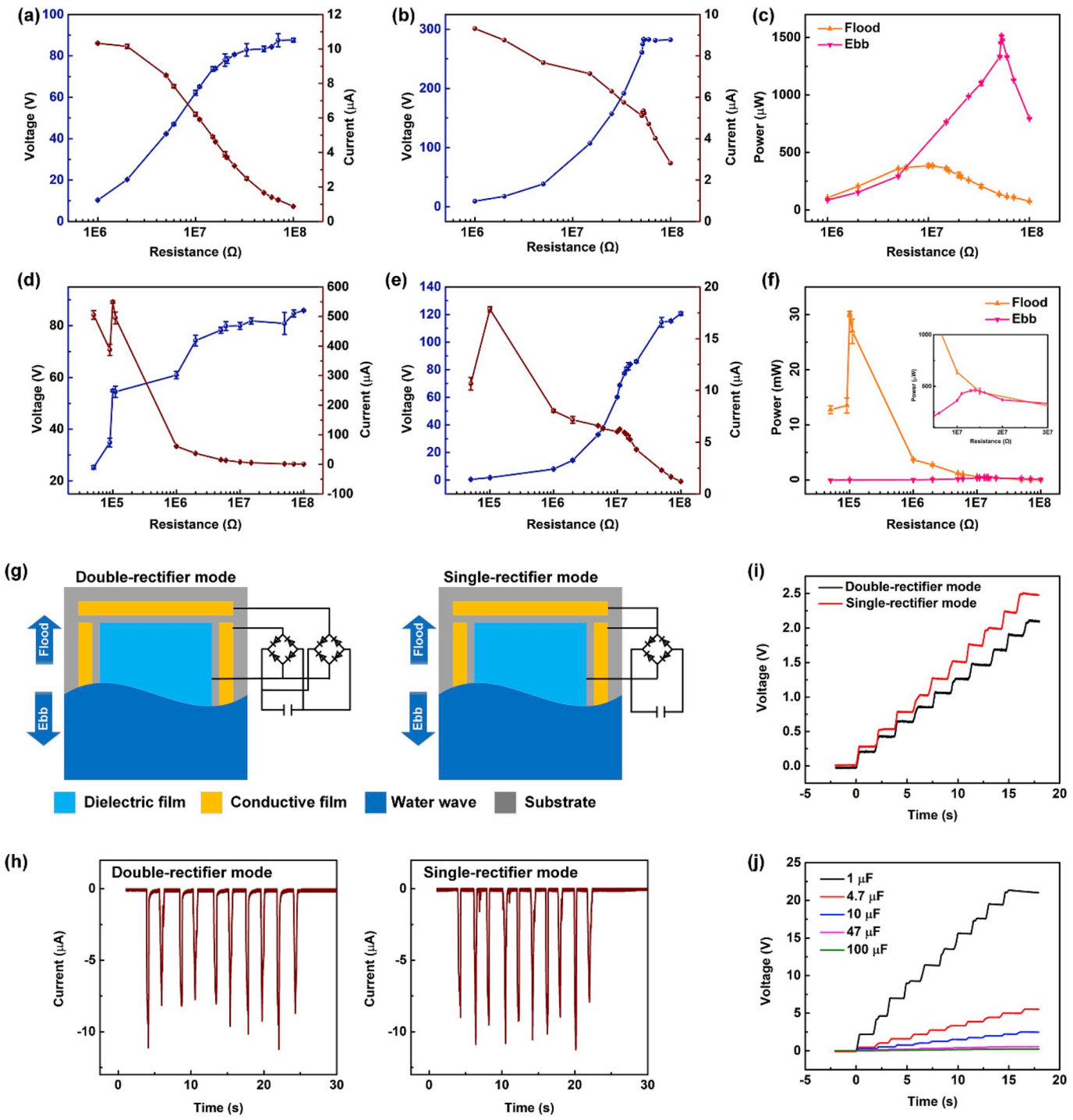

Fig. 5. (a) Dependence of voltage and current of the U-TENG in flood process on external resistive loads. (b) Dependence of voltage and current of the U-TENG in ebb process on external resistive loads. (c) Dependence of output power of the U-TENG in the flood process and the ebb process on external resistive loads. (d) Dependence of voltage and current of the B-TENG in flood process on resistive loads. (e) Dependence of voltage and current of the B-TENG in ebb process on external resistive loads. (f) Dependence of output power of the B-TENG in the flood process and the ebb process on external resistive loads. Insert is enlarged diagram to see the ebb power. (g) Rectifier circuit of Ū-TENG with Double-rectifier mode and Single-rectifier mode. (h) Rectified current of Ū-TENG with Double-rectifier mode and Single-rectifier mode. (i) Capacitor charge of 10 μF with Ū-TENG along Double-rectifier mode and Single-rectifier mode. (j) Capacitor charge of different capacity with Ū-TENG along Single-rectifier mode.

resistance load of 14 MΩ. These different values of output power in the flood and ebb process are attributed to instantaneously contact or non-contact with B electrode. All the above discussions show that U electrode and B electrode have different functions to support the Ū-TENG.

For further application, there are two modes of rectifier circuit about the U electrode, D electrode and B electrode, shown in Fig. 5g. Wherein, the double-rectifier mode refers that each electrode works with one rectifier, and the single-rectifier mode refers that two electrodes together work with one rectifier. The rectified currents of two modes are shown in Fig. 5h. Average rectified current of the double-rectifier mode is 9.22 μA, while average rectified current of the single-rectifier mode is 9.84 μA. Next in Fig. 5i, a capacitor of 10 μF is charged with these two

modes, and results show that after five cycles it can reach 2.11 V with the double-rectifier mode and 2.51 V with the single-rectifier mode. This difference is attributed to energy consumption in rectifier circuit and the single-rectifier mode shows superiority. Moreover, capacitors of 1 μF, 4.7 μF, 10 μF, 47 μF and 100 μF are charged in Fig. 5j with the single-rectifier mode, and final voltage can reach 21.35 V, 5.55 V, 2.51 V, 0.57 V and 0.25 V respectively. Therefore, it shows that the Ū-TENG can be effectively applied as blue energy harvester and convert wave energy into electric power.

2.3. Seashore IoT applications with Ū electrode triboelectric nanogenerator

The seashore area is an important part of production, ecology, transportation and research. Thus, understanding and utilization of seashore is a critical issue to human life. In recent years, the internet-of-things (IoT) have been rapidly developed to build a giant network of connected things and people. Various IoT applications based on triboelectric nanogenerator have been demonstrated to support Smart Home System, Wearable Technology and Human-Computer Interaction Techniques, but rare research works are discussed Seashore IoT Applications. Considering directly interaction with water waves, the Ū-TENG device can be applied as a thin film blue energy harvester and expand IoT applications aiming at seashore area.

First, a wave warning system is built and shown in Fig. 6a, where B electrode and D electrode access to current monitoring system. Based on orientation of water waves, once waves beyond the preset limit area and contact with B electrode, the wave warning system is triggered and an instantaneous strong current signal can be seen by the monitoring system, as shown in Fig. 6b. Thus, the wave level can be recorded for further analyze of dynamics sea or applied to warn people around seashore area.

Second, a continuously power system is introduced to support low power sensors. Shown in Fig. 6d, two mode of circuit connection methods are designed. When a low power temperature sensor is working with mode i, refer that the Ū-TENG fully output to power the sensor, this sensor shown in Fig. S3 and Video S2 is in overload state and displaying abnormally. This sensor can only work normally after the wave pump stops, and display temperature until electrical power is running out. When this sensor works with mode ii, refer that B electrode grounded to consume extra electric power, the sensor can be continuously working and displaying normally, as shown in Fig. 6e and Video S3. Therefore, the Ū-TENG device can sustain sensors working and collecting kinds of information.

Supplementary data related to this article can be found at https://doi.org/10.1016/j.nanoen.2019.104167.

Third, a wireless transmitter is applied to support a wireless transmission system. Results shown in Fig. 6f prove that a capacitor of 47 μF can be charged to 7 V within 50s with the Ū-TENG operated with wave pump. Based on the Ū-TENG, a wireless transmitter successfully sends out temperature and humidity signals to a mobile phone, shown in Fig. 6f and Video S4. This wireless signal transmission system is important for further seashore IoT applications, inspectors can obtain information from distributed signal transmitting station when they take an inspection tour of seashore area.

Supplementary data related to this article can be found at https://doi.org/10.1016/j.nanoen.2019.104167.

Moreover, the Ū-TENG applied as raindrop energy harvester has been discussed, shown in Fig. 6g and h. A simulation experiment is operating with a volume of 500 ml water flowing onto the Ū-TENG device. The rectified current in Fig. 6g shows that a significant current of 70 μA is obtained when the water drops firstly contact with the device. Then a constantly changing current is detected in the process of water drops continuously falling, and the average value is about 2.4 μA. Capacitors of 1 μF, 4.7 μF and10 μF are charged under water drops of 500 ml, the results shown in Fig. 6h indicates that final voltage can reach 5.06 V,1.32 V and 0.68 V respectively. So, the Ū-TENG device can also collect raindrop energy when a diverse climate occurs in seashore area.

The stability of Ū-TENG has been tested and shown in Fig. S4, the output voltage can retain 66.2% of initial output after 1000 cycles test and retain 50.2% of initial output after 5000 cycles test. And the output voltage can restore to 90.7% of initial output after gently wipe off residual water on the device. The performance of Ū-TENG with different salinity water has been tested and shown in Fig. S5. The output voltage can retain 72.6% of initial output with salinity water of 10‰, and 42.6% of initial output with salinity water of 35‰. It is worth mentioning that seawater in the world's oceans has a salinity of approximately 35‰, and the output performance can foresee the practical applications of the Ū-TENG as a blue energy harvester in seashore area.

3. Conclusion

In summary, a thin film blue energy harvester based on liquid-solid contact triboelectric nanogenerator is prepared. Final device is flexible and bendable, suitable for substrate with various seashore situations. And the fabrication process is facile and suit for further industrial

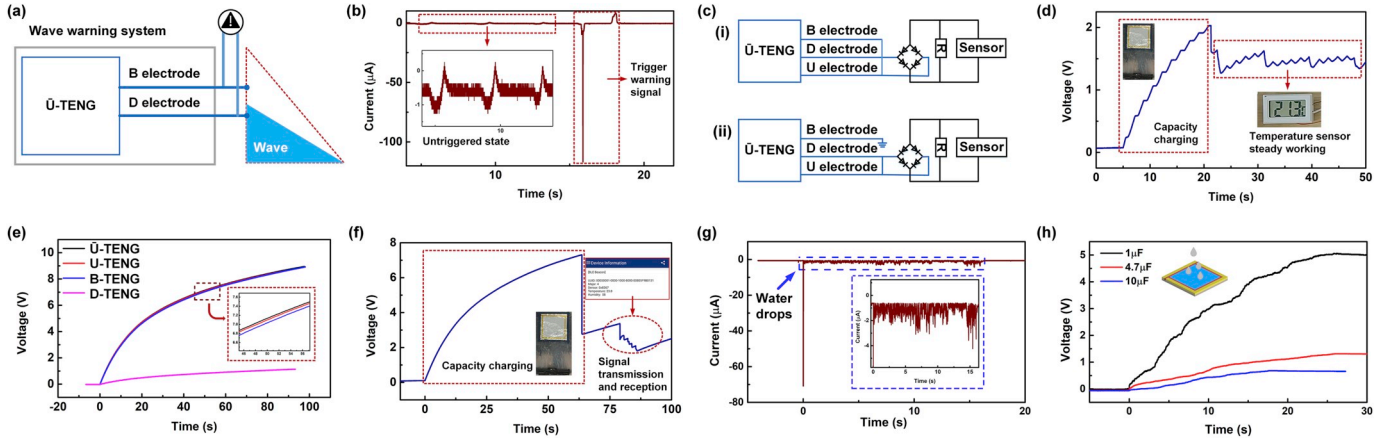

Fig. 6. (a) The schematic diagram of wave warning system operated with B electrode and D electrode. (b) Current variation of untriggered state and triggered state in the wave warning system. (c) Two different circuits for low power sensor. (d) A temperature sensor is powered and continuously working normal. (e) A capacitor of 47 μF is charged with Ū-TENG, U-TENG, B-TENG and D-TENG operated with wave pump. (f) A wireless transmitter is powered with Ū-TENG and environment signals successfully send to a mobile phone. A simulation experiment of Ū-TENG device applied as a raindrop energy harvester: (g) Rectified current under water drops, insert is an enlarge figure. (h) Different capacitor charging under water drops with volume of 500 ml.

production. With the structure of external Ū electrode including B electrode and U electrode, the shielding effect is hugely minimized, and outputs are effectively improved. Thus, the Ū-TENG can effectively extract power from waves' flood and ebb processes. Moreover, a seashore IoT system is built, which contains a wave warning system based on B electrode play as a safety switch, a continuously power system based on designed connection of Ū electrode, and a wireless transmission system based on a wireless transmitter. Therefore, this work provides a new kind of thin film blue energy harvester and expands IoT applications about seashore area.

4. Experimental section

4.1. Fabrication of the single electrode triboelectric nanogenerator

Firstly, a square of 22 cm × 22 cm is cut from a FEP (Fluorinated ethylene propylene) sheet with 50 μm thickness. Then a square of 20 cm × 20 cm is firstly cut from a roll of Aluminum foil with 10 μm thickness, and it is attached on backside of FEP film by electrostatic adsorption. Finally, this FEP with attached electrode is stacked on substrate of PVC (polyvinyl chloride soft film, 0.1 mm thickness, Alfa Packaging), with sealing silicone (Kafuter sealant) on backside and sealing tape (Kapton tape) on frontside.

4.2. Fabrication of the Ū electrode triboelectric nanogenerator

Based on prepared single electrode triboelectric nanogenerator, external Ū electrode is added. Firstly, Aluminum tape of 15 mm width is chosen to cover edges of the single triboelectric nanogenerator. Then a piece of Aluminum tape with 23 cm length is attached on upper edge with approximate 1 mm gap from edge of back electrode, this piece of Aluminum tape is applied as Bar electrode. Similarly, pieces of Aluminum tape are combined into U-shape and attached around left, bottom and right edges with approximate 0.5 mm gap, these pieces of Aluminum tape are applied as U-shape electrode.

4.3. Characterization and electrical measurement

The outputs of triboelectric nanogenerator are measured by Model 6514 Electrometer (Keithley), and experiments' data is acquired and saved by Model DSOX3034T Oscilloscope (Keysight). Application experiments are operated with wave pump (Laoyujiang) equipped on bottom of box (length of 70 cm, width of 52 cm, height of 43 cm).

Acknowledgements

This work was supported by: HIFES Seed Funding-2017-01 grant (R263-501-012-133) "Hybrid Integration of Flexible Power Source and Pressure Sensors" at the National University of Singapore; Singapore-Poland Joint Grant (R-263-000-C91-305) "Chip-Scale MEMS Micro-Spectrometer for Monitoring Harsh Industrial Gases" by Agency for Science, Technology and Research (A*STAR), Singapore and NAWA"Academic International Partnerships of Wroclaw University of Science and technology" programme by Polish National Agency for Academic Exchange Programme.

Appendix A. Supplementary data

Supplementary data to this article can be found online at https://doi.org/10.1016/j.nanoen.2019.104167.

References

[1] J.A. Turner, A realizable renewable energy future, Science 285 (1999) 687–689.
[2] D. Gielen, F. Boshell, D. Saygin, Climate and energy challenges for materials science, Nat. Mater. 15 (2016) 117–120.
[3] Q. Schiermeier, J. Tollefson, T. Scully, A. Witze, O. Morton, Electricity without carbon, Nature 454 (2008) 816.
[4] J. Tollefson, Power from the oceans: blue energy, Nature 508 (2014) 302–304.
[5] S.H. Salter, Wave power, Nature 249 (1974) 720–724.
[6] A.F.d.O. Falcão, Wave energy utilization: a review of the technologies, Renew. Sustain. Energy Rev. 14 (2010) 899–918.
[7] J. Falnes, A review of wave-energy extraction, Mar. Struct. 20 (2007) 185–201.
[8] A. Cho, To catch a wave, Science (New York, N.Y.) 347 (2015) 1084–1088.
[9] E. Callaway, Energy: to catch a wave, Nature 450 (2007) 156–159.
[10] M.A. Mustapa, O.B. Yaakob, Y.M. Ahmed, C.-K. Rheem, K.K. Koh, F.A. Adnan, Wave energy device and breakwater integration: a review, Renew. Sustain. Energy Rev. 77 (2017) 43–58.
[11] R. Tiron, F. Mallon, F. Dias, E.G. Reynaud, The challenging life of wave energy devices at sea: a few points to consider, Renew. Sustain. Energy Rev. 43 (2015) 1263–1272.
[12] J. Scruggs, P. Jacob, Harvesting ocean wave energy, Science 323 (2009) 1176–1178.
[13] Z.L. Wang, S. Wang, L. Lin, Triboelectric nanogenerators as self-powered active sensors, Nano Energy 11 (2015) 436–462.
[14] J. Chen, Z.L. Wang, Reviving vibration energy harvesting and self-powered sensing by a triboelectric nanogenerator, Joule 1 (2017) 480–521.
[15] Z. Lin, J. Chen, J. Yang, Recent progress in triboelectric nanogenerators as a renewable and sustainable power source, J. Nanomater. (2016) 1–24, 2016.
[16] Z.L. Wang, T. Jiang, L. Xu, Toward the blue energy dream by triboelectric nanogenerator networks, Nano Energy 39 (2017) 9–23.
[17] Z.L. Wang, J. Chen, L. Lin, Progress in triboelectric nanogenerators as a new energy technology and self-powered sensors, Energy Environ. Sci. 8 (2015) 2250–2282.
[18] C. Wu, A.C. Wang, W. Ding, H. Guo, Z.L. Wang, Triboelectric nanogenerator: a foundation of the energy for the new era, Adv. Energy Mater. 9 (2019), 1802906-n/a.
[19] Z.L. Wang, On Maxwell's displacement current for energy and sensors: the origin of nanogenerators, Mater. Today 20 (2017) 74–82.
[20] C. Xu, Y. Zi, A.C. Wang, H. Zou, Y. Dai, X. He, P. Wang, Y.C. Wang, P. Feng, D. Li, Z. L. Wang, On the electron-transfer mechanism in the contact-electrification effect, Adv. Mater. 30 (2018) e1706790-n/a.
[21] S. Lin, L. Xu, C. Xu, X. Chen, A.C. Wang, B. Zhang, P. Lin, Y. Yang, H. Zhao, Z. L. Wang, Electron transfer in nanoscale contact electrification: effect of temperature in the metal–dielectric case, Adv. Mater. 31 (2019) e1808197-n/a.
[22] C. Xu, B. Zhang, A.C. Wang, H. Zou, G. Liu, W. Ding, C. Wu, M. Ma, P. Feng, Z. Lin, Z.L. Wang, Contact-electrification between two identical materials: curvature effect, ACS Nano 13 (2019) 2034–2041.
[23] P. Bai, G. Zhu, Z.-H. Lin, Q. Jing, J. Chen, G. Zhang, J. Ma, Z.L. Wang, Integrated multilayered triboelectric nanogenerator for harvesting biomechanical energy from human motions, ACS Nano 7 (2013) 3713–3719.
[24] S. Wang, Y. Xie, S. Niu, L. Lin, Z.L. Wang, Freestanding triboelectric-layer-based nanogenerators for harvesting energy from a moving object or human motion in contact and non-contact modes, Adv. Mater. 26 (2014) 2818–2824.
[25] L. Liu, W. Tang, C. Deng, B. Chen, K. Han, W. Zhong, Z.L. Wang, Self-powered versatile shoes based on hybrid nanogenerators, Nano Res. 11 (2018) 3972–3978.
[26] M. Zhu, Q. Shi, T. He, Z. Yi, Y. Ma, B. Yang, T. Chen, C. Lee, Self-powered and self-functional cotton sock using piezoelectric and triboelectric hybrid mechanism for healthcare and sports monitoring, ACS Nano 13 (2019) 1940–1952.
[27] J. Ma, Y. Jie, J. Bian, T. Li, X. Cao, N. Wang, From triboelectric nanogenerator to self-powered smart floor: a minimalist design, Nano Energy 39 (2017) 192–199.
[28] L. Gao, D. Hu, M. Qi, J. Gong, H. Zhou, X. Chen, J. Chen, J. Cai, L. Wu, N. Hu, Y. Yang, X. Mu, A double-helix-structured triboelectric nanogenerator enhanced with positive charge traps for self-powered temperature sensing and smart-home control systems, Nanoscale 10 (2018) 19781–19790.
[29] Q. Shi, C. Qiu, T. He, F. Wu, M. Zhu, J.A. Dziuban, R. Walczak, M.R. Yuce, C. Lee, Triboelectric single-electrode-output control interface using patterned grid electrode, Nano Energy 60 (2019) 545–556.
[30] T. He, Z. Sun, Q. Shi, M. Zhu, D.V. Anaya, M. Xu, T. Chen, M.R. Yuce, A.V.-Y. Thean, C. Lee, Self-powered glove-based intuitive interface for diversified control applications in real/cyber space, Nano Energy 58 (2019) 641–651.
[31] Q. Shi, C. Lee, Self-powered bio-inspired spider-net-coding interface using single-electrode triboelectric nanogenerator, Adv. Sci. (2019) 1900617.
[32] W. Yang, J. Chen, G. Zhu, J. Yang, P. Bai, Y. Su, Q. Jing, X. Cao, Z.L. Wang, Harvesting energy from the natural vibration of human walking, ACS Nano 7 (2013) 11317–11324.
[33] L. Liu, W. Tang, B. Chen, C. Deng, W. Zhong, X. Cao, Z.L. Wang, A self-powered portable power bank based on a hybridized nanogenerator, Adv. Mater. Technol. 3 (2018) 1700209.
[34] J. Chen, G. Zhu, W. Yang, Q. Jing, P. Bai, Y. Yang, T.C. Hou, Z.L. Wang, Harmonic-resonator-based triboelectric nanogenerator as a sustainable power source and a self-powered active vibration sensor, Adv. Mater. 25 (2013) 6094–6099.
[35] H. Zhang, Y. Yang, Y. Su, J. Chen, K. Adams, S. Lee, C. Hu, Z.L. Wang, Triboelectric nanogenerator for harvesting vibration energy in full space and as self-powered acceleration sensor, Adv. Funct. Mater. 24 (2014) 1401–1407.
[36] C. Wu, R. Liu, Z.L. Wang, J. Wang, Y. Zi, L. Lin, A spring-based resonance coupling for hugely enhancing the performance of triboelectric nanogenerators for harvesting low-frequency vibration energy, Nano Energy 32 (2017) 287–293.
[37] S. Chen, C. Gao, W. Tang, H. Zhu, Y. Han, Q. Jiang, T. Li, X. Cao, Z. Wang, Self-powered cleaning of air pollution by wind driven triboelectric nanogenerator, Nano Energy 14 (2015) 217–225.

[38] M.-L. Seol, J.-H. Woo, S.-B. Jeon, D. Kim, S.-J. Park, J. Hur, Y.-K. Choi, Vertically stacked thin triboelectric nanogenerator for wind energy harvesting, Nano Energy 14 (2015) 201–208.
[39] B. Chen, Y. Yang, Z.L. Wang, Scavenging wind energy by triboelectric nanogenerators, Adv. Energy Mater. 8 (2018) 1702649–n/a.
[40] Z.-H. Lin, G. Cheng, W. Wu, K.C. Pradel, Z.L. Wang, Dual-mode triboelectric nanogenerator for harvesting water energy and as a self-powered ethanol nanosensor, ACS Nano 8 (2014) 6440–6448.
[41] Y. Liu, N. Sun, J. Liu, Z. Wen, X. Sun, S.-T. Lee, B. Sun, Integrating a silicon solar cell with a triboelectric nanogenerator via a mutual electrode for harvesting energy from sunlight and raindrops, ACS Nano 12 (2018) 2893–2899.
[42] L. Zheng, Z.-H. Lin, G. Cheng, W. Wu, X. Wen, S. Lee, Z.L. Wang, Silicon-based hybrid cell for harvesting solar energy and raindrop electrostatic energy, Nano Energy 9 (2014) 291–300.
[43] H.R. Zhu, W. Tang, C.Z. Gao, Y. Han, T. Li, X. Cao, Z.L. Wang, Self-powered metal surface anti-corrosion protection using energy harvested from rain drops and wind, Nano Energy 14 (2015) 193–200.
[44] Q. Liang, X. Yan, X. Liao, Y. Zhang, Integrated multi-unit transparent triboelectric nanogenerator harvesting rain power for driving electronics, Nano Energy 25 (2016) 18–25.
[45] Y.-C. Lai, Y.-C. Hsiao, H.-M. Wu, Z.L. Wang, Waterproof fabric-based multifunctional triboelectric nanogenerator for universally harvesting energy from raindrops, wind, and human motions and as self-powered sensors, Adv. Sci. 6 (2019) 1801883.
[46] Z.-H. Lin, G. Cheng, S. Lee, K.C. Pradel, Z.L. Wang, Harvesting water drop energy by a sequential contact-electrification and electrostatic-induction process, Adv. Mater. 26 (2014) 4690–4696.
[47] X. Wang, S. Niu, Y. Yin, F. Yi, Z. You, Z.L. Wang, Triboelectric nanogenerator based on fully enclosed rolling spherical structure for harvesting low-frequency water wave energy, Adv. Energy Mater. 5 (2015), 1501467-n/a.
[48] L. Xu, T. Jiang, P. Lin, J.J. Shao, C. He, W. Zhong, X.Y. Chen, Z.L. Wang, Coupled triboelectric nanogenerator networks for efficient water wave energy harvesting, ACS Nano 12 (2018) 1849–1858.
[49] Q. Shi, H. Wang, H. Wu, C. Lee, Self-powered triboelectric nanogenerator buoy ball for applications ranging from environment monitoring to water wave energy farm, Nano Energy 40 (2017) 203–213.
[50] G. Zhu, Y. Su, P. Bai, J. Chen, Q. Jing, W. Yang, Z.L. Wang, Harvesting water wave energy by asymmetric screening of electrostatic charges on a nanostructured hydrophobic thin-film surface, ACS Nano 8 (2014) 6031–6037.
[51] X.J. Zhao, G. Zhu, Y.J. Fan, H.Y. Li, Z.L. Wang, Triboelectric charging at the nanostructured solid/liquid interface for area-scalable wave energy conversion and its use in corrosion protection, ACS Nano 9 (2015) 7671–7677.
[52] X.J. Zhao, S.Y. Kuang, Z.L. Wang, G. Zhu, Highly adaptive solid–liquid interfacing triboelectric nanogenerator for harvesting diverse water wave energy, ACS Nano 12 (2018) 4280–4285.
[53] X. Li, J. Tao, W. Guo, X. Zhang, J. Luo, M. Chen, J. Zhu, C. Pan, A self-powered system based on triboelectric nanogenerators and supercapacitors for metal corrosion prevention, J. Mater. Chem. 3 (2015) 22663–22668.
[54] X. Li, J. Tao, J. Zhu, C. Pan, A nanowire based triboelectric nanogenerator for harvesting water wave energy and its applications, Apl. Mater. 5 (2017), 074104.
[55] X. Li, J. Tao, X. Wang, J. Zhu, C. Pan, Z.L. Wang, Networks of high performance triboelectric nanogenerators based on liquid–solid interface contact electrification for harvesting low-frequency blue energy, Advanced Energy Materials 8 (2018), 1800705-n/a.
[56] M. Xu, S. Wang, S.L. Zhang, W. Ding, P.T. Kien, C. Wang, Z. Li, X. Pan, Z.L. Wang, A highly-sensitive wave sensor based on liquid-solid interfacing triboelectric nanogenerator for smart marine equipment, Nano Energy 57 (2019) 574–580.
[57] Z.-H. Lin, G. Cheng, L. Lin, S. Lee, Z.L. Wang, Water–solid surface contact electrification and its use for harvesting liquid-wave energy, Angew. Chem. Int. Ed. 52 (2013) 12545–12549.
[58] W. Tang, B.D. Chen, Z.L. Wang, Recent progress in power generation from water/liquid droplet interaction with solid surfaces, Adv. Funct. Mater. 0 (2019) 1901069.
[59] L. Pan, J. Wang, P. Wang, R. Gao, Y.-C. Wang, X. Zhang, J.-J. Zou, Z.L. Wang, Liquid-FEP-based U-tube triboelectric nanogenerator for harvesting water-wave energy, Nano Research 11 (2018) 4062–4073.
[60] C. Hou, T. Chen, Y. Li, M. Huang, Q. Shi, H. Liu, L. Sun, C. Lee, A rotational pendulum based electromagnetic/triboelectric hybrid-generator for ultra-low-frequency vibrations aiming at human motion and blue energy applications, Nano Energy 63 (2019) 103871.
[61] X. Liang, T. Jiang, G. Liu, T. Xiao, L. Xu, W. Li, F. Xi, C. Zhang, Z.L. Wang, Triboelectric nanogenerator networks integrated with power management module for water wave energy harvesting, Adv. Funct. Mater. (2019) 1807241.
[62] X. Yang, L. Xu, P. Lin, W. Zhong, Y. Bai, J. Luo, J. Chen, Z.L. Wang, Macroscopic self-assembly network of encapsulated high-performance triboelectric nanogenerators for water wave energy harvesting, Nano Energy 60 (2019) 404–412.
[63] P. Cheng, H. Guo, Z. Wen, C. Zhang, X. Yin, X. Li, D. Liu, W. Song, X. Sun, Z. L. Wang, J. Wang, Largely enhanced triboelectric nanogenerator for efficient harvesting of water wave energy by soft contacted structure, Nano Energy 57 (2019) 432–439.
[64] T. Jiang, Y. Yao, L. Xu, L. Zhang, T. Xiao, Z.L. Wang, Spring-assisted triboelectric nanogenerator for efficiently harvesting water wave energy, Nano Energy 31 (2017) 560–567.
[65] Y. Xi, J. Wang, Y. Zi, X. Li, C. Han, X. Cao, C. Hu, Z. Wang, High efficient harvesting of underwater ultrasonic wave energy by triboelectric nanogenerator, Nano Energy 38 (2017) 101–108.
[66] H. Yang, M. Deng, Q. Tang, W. He, C. Hu, Y. Xi, R. Liu, Z.L. Wang, A nonencapsulative pendulum-like paper–based hybrid nanogenerator for energy harvesting, Adv. Energy Mater. 0 (2019) 1901149.
[67] S.L. Zhang, M. Xu, C. Zhang, Y.-C. Wang, H. Zou, X. He, Z. Wang, Z.L. Wang, Rationally designed sea snake structure based triboelectric nanogenerators for effectively and efficiently harvesting ocean wave energy with minimized water screening effect, Nano Energy 48 (2018) 421–429.
[68] G. Liu, H. Guo, S. Xu, C. Hu, Z.L. Wang, Oblate spheroidal triboelectric nanogenerator for all-weather blue energy harvesting, Adv. Energy Mater. 9 (2019) 1900801.
[69] M. Xu, T. Zhao, C. Wang, S.L. Zhang, Z. Li, X. Pan, Z.L. Wang, High power density tower-like triboelectric nanogenerator for harvesting arbitrary directional water wave energy, ACS Nano 13 (2019) 1932–1939.
[70] Z. Wen, H. Guo, Y. Zi, M.-H. Yeh, X. Wang, J. Deng, J. Wang, S. Li, C. Hu, L. Zhu, Z. L. Wang, Harvesting broad frequency band blue energy by a triboelectric–electromagnetic hybrid nanogenerator, ACS Nano 10 (2016) 6526–6534.
[71] H. Shao, P. Cheng, R. Chen, L. Xie, N. Sun, Q. Shen, X. Chen, Q. Zhu, Y. Zhang, Y. Liu, Z. Wen, X. Sun, Triboelectric–electromagnetic hybrid generator for harvesting blue energy, Nano-Micro Lett. 10 (2018) 54.
[72] P. Cheng, Y. Liu, Z. Wen, H. Shao, A. Wei, X. Xie, C. Chen, Y. Yang, M. Peng, Q. Zhuo, X. Sun, Atmospheric pressure difference driven triboelectric nanogenerator for efficiently harvesting ocean wave energy, Nano Energy 54 (2018) 156–162.
[73] Z.L. Wang, New wave power, Nature 542 (2017) 159.
[74] Y. Zi, H. Guo, Z. Wen, M.-H. Yeh, C. Hu, Z.L. Wang, Harvesting low-frequency (<5 Hz) irregular mechanical energy: a possible killer application of triboelectric nanogenerator, ACS Nano 10 (2016) 4797–4805.
[75] C. Zhang, W. Tang, C. Han, F. Fan, Z.L. Wang, Theoretical comparison, equivalent transformation, and conjunction operations of electromagnetic induction generator and triboelectric nanogenerator for harvesting mechanical energy, Adv. Mater. 26 (2014) 3580–3591.
[76] F.-R. Fan, W. Tang, Y. Yao, J. Luo, C. Zhang, Z.L. Wang, Complementary power output characteristics of electromagnetic generators and triboelectric generators, Nanotechnology 25 (2014) 135402.
[77] H.-X. Zhang, X.-S. Zhang, M.-D. Han, R.-X. Wang, W. Wang, B. Meng, F.-Y. Zhu, X.-M. Sun, W. Hu, Z.-H. Li, High-performance triboelectric nanogenerator with enhanced energy density based on single-step fluorocarbon plasma treatment, Nano Energy 4 (2014) 123–131.
[78] V. Nguyen, R. Yang, Effect of humidity and pressure on the triboelectric nanogenerator, Nano Energy 2 (2013) 604–608.
[79] H. Zhang, Y. Yang, Y. Su, J. Chen, C. Hu, Z. Wu, Y. Liu, C. Ping Wong, Y. Bando, Z. L. Wang, Triboelectric nanogenerator as self-powered active sensors for detecting liquid/gaseous water/ethanol, Nano Energy 2 (2013) 693–701.
[80] Z.L. Wang, Triboelectric nanogenerators as new energy technology and self-powered sensors - principles, problems and perspectives, Faraday Discuss 176 (2015) 447–458.
[81] D.C. Grahame, The electrical double layer and the theory of electrocapillarity, Chem. Rev. 41 (1947) 441–501.
[82] R. Parsons, Electrical double-layer - recent experimental and theoretical developments, Chem. Rev. 90 (1990) 813–826.
[83] Z.L. Wang, Entropy theory of distributed energy for internet of things, Nano Energy 58 (2019) 669–672.
[84] S.-B. Jeon, Y.-H. Nho, S.-J. Park, W.-G. Kim, I.-W. Tcho, D. Kim, D.-S. Kwon, Y.-K. Choi, Self-powered fall detection system using pressure sensing triboelectric nanogenerators, Nano Energy 41 (2017) 139–147.
[85] K.-W. Lim, M. Peddigari, C.H. Park, H.Y. Lee, Y. Min, J.-W. Kim, C.-W. Ahn, J.-J. Choi, B.-D. Hahn, J.-H. Choi, D.-S. Park, J.-K. Hong, J.-T. Yeom, W.-H. Yoon, J. Ryu, S.N. Yi, G.-T. Hwang, A high output magneto-mechano-triboelectric generator enabled by accelerated water-soluble nano-bullets for powering a wireless indoor positioning system, Energy Environ. Sci. 12 (2019) 666–674.
[86] W. Li, G. Liu, D. Jiang, C. Wang, W. Li, T. Guo, J. Zhao, F. Xi, W. Liu, C. Zhang, Interdigitated electrode-based triboelectric sliding sensor for security monitoring, Adv. Mater. Technol. 3 (2018) 1800189.
[87] K. Dong, X. Peng, Z.L. Wang, Fiber/fabric-based piezoelectric and triboelectric nanogenerators for flexible/stretchable and wearable electronics and artificial intelligence, Adv. Mater. 0 (2019) 1902549.
[88] A. Oron, S.H. Davis, S.G. Bankoff, Long-scale evolution of thin liquid films, Rev. Mod. Phys. 69 (1997) 931–980.
[89] L.Y. Yeo, H.C. Chang, Static and spontaneous electrowetting, Mod. Phys. Lett. B 19 (2005) 549–569.

Long Liu received his Ph.D. degree from Beijing Institute of Nano energy and Nanosystems, Chinese Academy of Sciences in 2018. He is currently a Research Fellow in the Department of Electrical and Computer Engineering, National University of Singapore. His research interests are focused on energy harvesters and self-powered sensors.

Qiongfeng Shi received his B.Eng. degree from the Department of Electronic Engineering and Information Science, University of Science and Technology of China (USTC) in 2012, and received his Ph.D. degree from the Department of Electrical and Computer Engineering, National University of Singapore (NUS) in 2018. He is currently a Research Fellow in the Department of Electrical and Computer Engineering, National University of Singapore. His research interests include energy harvesters, triboelectric nanogenerators, self-powered sensors, and wearable/implantable electronics.

John S. Ho received his PhD in electrical engineering at Stanford University where he was a National Defense Science and Engineering Graduate Fellow. Currently, he is an assistant professor in the Department of Electrical and Computer Engineering at the National University of Singapore. His current research interests are centered on the development of wireless technologies for miniaturized bioelectronic devices and their application to human health.

Chengkuo Lee received his Ph.D. degree in Precision Engineering from The University of Tokyo in 1996. Currently, he is the director of Center for Intelligent Sensors and MEMS at National University of Singapore, Singapore. In 2001, he cofounded Asia Pacific Microsystems, Inc., where he was the Vice President. From 2006 to 2009, he was a Senior Member of the Technical Staff at the Institute of Microelectronics, A-STAR, Singapore. He has contributed to more than 300 peer-reviewed international journal articles.